Available online at www.sciencedirect.com
SCIENCE DIRECT®
Optics Communications 246 (2005) 303–311
OPTICS COMMUNICATIONS
www.elsevier.com/locate/optcom

Chromatic dispersion fluctuations in optical fibers due to temperature and its effects in high-speed optical communication systems

Paulo S. André *, Armando N. Pinto

Institute of Telecommunications, University of Aveiro, Campus de Santiago, 3810-193 Aveiro, Portugal
Physics Department, University of Aveiro, Campus de Santiago, 3810-193 Aveiro, Portugal
Electronic and Telecommunications Department, University of Aveiro, Campus de Santiago, 3810-193 Aveiro, Portugal

Received 7 July 2004; received in revised form 10 October 2004; accepted 4 November 2004

Abstract

Several research groups have been proposing different dispersion compensation schemes, for very high-speed ($\geqslant$40 Gbit/s) long-haul systems operating in the C-band window (1530–1563 nm) over standard single mode fibers, known as ITU-T G.652 fibers. The focus on these high chromatic dispersion fibers is due to the large amount of standard single mode fibers already installed in the field. Although several dispersion compensation techniques have proved to be successful, the long term stability of this kind of systems remains to be seen. In fact, when in the field, these high speed systems present a very unstable behavior, which is translated in large variations of the bit error rate. In order to stabilize the systems strong forward error correction codes have been used. In this work, we prove quantitatively that this inherent instability is mainly due to chromatic dispersion variations induced by temperature swings. Two models for the chromatic dispersion and chromatic dispersion slope variations with temperature are developed and validated using laboratory measurements previously published. After the effect of temperature change is analyzed in terms of eye opening penalty, it is shown that for systems operating at 40 Gbit/s and above temperature effects have to be considered in system design.

PACS: 42.79.S; 78.20.C; 42.81
Keywords: Optical communication systems; Refractive index; Optical fibers

1. Introduction

TRAFFIC demand has been increasing steadily in the last few years. In order to support this

* Corresponding author. Tel.: +351 2343 77900; fax: +351 2343 77901.
E-mail addresses: pandre@av.it.pt (P.S. André), anp@det.ua.pt (A.N. Pinto).

0030-4018/$ - see front matter
doi:10.1016/j.optcom.2004.11.017

increasing traffic demand the optical links between the main cities, which are typically terrestrial links with hundreds of kilometers operating at 10 Git/s per channel, have to be upgraded. A solution for the upgrading of these links is to increase the bit rate per channel to 40, 80 or even to 160 Gbit/s. The major operators intend to use the already installed cables to support these high speed systems, which is not surprising, as the most cost effective solution usually resides in upgrading the terminal equipment keeping the link unchanged.

However, the majority of the cables in the field contain G.652 fibers, which have a high level of chromatic dispersion in the conventional spectral window, where erbium doped fiber amplifiers provide the optical gain. In high bit rate systems, in order to cope with tight restrictions imposed by chromatic dispersion, it is mandatory to use dispersion compensation techniques. Several devices and schemes have been proposed to provide an accurate management of the chromatic dispersion, over a large spectral window. However, even with wavelength per wavelength careful tuning, these systems still present an unstable behavior when tested in the field subjected to extreme environmental conditions. In order to maintain the bit error rate as low as 10^{-15}, systems designers have been using strong forward error correction codes. In this work, we account for the fundamental reason behind this unstable behavior.

Some authors have already attributed this unstable behavior to chromatic dispersion fluctuations induced by temperature variations. However, this problem is far from being completely solved. The earlier studies were mainly based on the previous notion that very high speed systems have to operate around the zero dispersion wavelength (λ_0). Hence, the focus was on the variation with temperature of the zero dispersion wavelength and on the dispersion around λ_0. However, the modern dispersion compensation devices and techniques allow these high speed systems to tolerate much higher levels of local chromatic dispersion [1].

In previous studies, the classical oscillator Lorentz's model, from which the Sellmeier's formula can be derived, have been largely used to consider the material refraction index variations with frequency and temperature.

In the studies presented by Hatton et al. [2] and Kim et al. [3] it was shown that the variation of λ_0 with the temperature ($d\lambda_0/dT$) is largely determine by the fiber's material. It was also shown in [2] for non-dispersion shifted fibers that, for pure silica and GeO_2 doped silica core fibers, the relation between the change in the zero dispersion wavelength and temperature variations is almost linear and around 0.025 nm/°C, for temperatures below 150 °C. A value slightly high, 0.030 nm/°C, was obtained by Kim et al. [3] for dispersion shifted fibers. In [3] the variation of λ_0 with the temperature was also analyzed using a two-term Sellmeier formalism, where all electronic oscillators were lumped into one effective term, and all lattice vibrational oscillators into another. It was found in [3] that the temperature dependence of λ_0 is mainly due to a −0.4 meV/°C temperature shift of the electronic Sellmeier band gap.

The study of the temperature dependence of the Sellmeir coefficients was also done in [4–6], respectively, by Lines, Matsuoka et al. and Ghosh et al. In [4] a microscopic analysis based on solid-state theory was done about the origin of the temperature dependence of the Sellmeier coefficients and a theoretical value was obtained in close agreement with the experimental one. It was also pointed out in [4] that the shift in the electronic resonance frequency contributes more than 95% of the material dispersion variation with temperature around the material zero dispersion wavelength. In [5], instead of lumping all the electronic oscillators into one effective term, two electronic resonance frequencies were considered. One to account for an exciton transition, with a resonance energy around 10.4 eV, and another to account for a band-to-band transition with a resonance energy around 11.6 eV.

In [7,8] a physically meaningful model for the temperature dependent refraction index of fused silica was presented by Ghosh. According to Ghosh, the variation due to temperature of the refraction index of fused silica can be described considering two terms, one related to the material thermal expansion and another related to the electronic resonance energy. The thermal expansion related term gives a negative contribution for the variation of the refraction index with temperature, as the material gets less dense. The term related to the shift of the electronic transition gives a positive contribution generally higher than the previous one.

Kato et al. [9] measured the chromatic dispersion of various types of optical fibers from 1535 to 1585 nm at different temperatures. They showed based on measurements that the chromatic dispersion slope and the chromatic dispersion thermal coefficient, defined as the variation of the dispersion with temperature, are correlated. Fibers with small dispersion slope presented also a small chromatic dispersion thermal coefficient. However, this conclusion seems not to apply always to fibers with high dispersion and dispersion slope governed by supermode coupling, as the dispersion compensation fibers (DCFs), as was pointed out by Schneider [10]. However, the results presented by Schneider were not confirmed by Rathje et al. [11], leaving the study of the thermal coefficient for DCFs as an open subject. Nevertheless, it seems that some DCFs present a positive thermal dispersion coefficient which can be used to counterbalance transmission fibers with a negative thermal coefficient. This was the support idea of the dynamically chromatic dispersion compensation scheme presented in [12].

Hamp et al. [13] measured the chromatic dispersion for different kind of fibers for several temperatures, and reached the conclusion that the dispersion slope at the zero dispersion wavelength depends significantly on temperature and this dependence should not be ignored to estimate the chromatic dispersion thermal effect for wavelengths far away from the zero dispersion wavelength.

In [14,15], the implications of temperature in single-mode fibers and high-speed systems, 40 and 80 Gbit/s, were analyzed.

In this full-length paper, two different approaches to model the chromatic dispersion dependence with temperature are in detail presented and compared. The first model is a more fundamental one in the sense that it is based on modeling the change in the interaction between light and matter with temperature. The second one is based on a heuristic expression for the chromatic dispersion. As we will show both models present quite accurate results. Using these models, values for chromatic dispersion and chromatic dispersion slope variations with temperature for standard single mode fibers, valid for the C-band, where erbium doped fiber amplifiers provide optical gain, are obtained. These values are validated by means of comparing with the measurements taken in [13]. High speed systems operating in the C-band, over standard single mode fibers which have the zero dispersion wavelength around 1315 nm are analyzed. The results obtained show clearly the importance of considering the effects of temperature in high speed optical communication systems design.

2. Group velocity dispersion in single-mode optical fibers

The refractive index of a material is the ratio of the speed of light in vacuum to the speed of light in the material. The variation of the refractive index with the frequency of the incident light constitutes the phenomenon of material dispersion. At the present time, the more complete description of the interaction between light and matter is given by the quantum theory of light. Hence, for a full account of the dispersion of light it would be necessary to go deeply into the atomic theory of matter. However, it is possible to describe the dispersion of light with a reasonable accuracy by the use of a classical model, mainly due to H.A. Lorentz, by considering the material response similar to the response of m harmonic oscillators.

2.1. A detailed model for chromatic dispersion

The classical Lorentz's oscillator model is able to account for electronic transitions and lattice vibrations, which are the dominant effects in materials where free carrier effects are negligible. Based on the oscillators Lorentz's model, an expression, usually called the Sellmeier formula, for the refractive index, n, valid for low loss materials and for optical wavelengths, λ, far from the material resonances, can be obtained [16]

$$n^2 - 1 = \sum_{k=1}^{m} \frac{A_k \lambda^2}{\lambda^2 - \lambda_k^2}, \tag{1}$$

where A_k is directly proportional to the number of oscillators per unit of volume and to the square of λ_k, which is the vacuum resonant wavelength associated with the kth resonance frequency of the material. For silica, a three-term Sellmeier expression is in general used, considering a resonance in the infrared, accounting for lattice vibrations, and two in the ultraviolet, accounting for electronic transitions. Values for the three A_k and λ_k coefficients have been experimentally estimated for pure and doped silica, see for example [16].

The group material dispersion parameter, $D_m(\lambda)$ can be directly obtained from (1)

$$D_m(\lambda) \equiv \frac{dt_g}{d\lambda} = \frac{1}{c}\frac{dN}{d\lambda} = -\frac{\lambda}{c}\frac{d^2 n}{d\lambda^2}, \tag{2}$$

where t_g is the group delay over a unit of distance, λ is the free-space wavelength and N is the group index of the material.

In order to evaluate the group dispersion parameter, $D(\lambda)$, in single-mode optical fibers, besides the material dispersion, it is also necessary to account for dispersive effects that arise from waveguiding.

In this work, we are going to consider only single-mode step-index fibers, however, the theoretical analysis can in principle be generalized for others fiber profiles, by means of considering an "equivalent" step-index profile [16].

For single-step single-mode optical fibers the group dispersion parameter is usually written as the summation of three terms, referred as the composite material dispersion, $D_{cm}(\lambda)$; waveguide dispersion, $D_w(\lambda)$; and profile dispersion, $D_p(\lambda)$ [16].

$$D(\lambda) = D_{cm}(\lambda) + D_w(\lambda) + D_p(\lambda). \tag{3}$$

In order to estimate the dispersion in single-mode fibers, a few approximations are usually done, which simplify the final expression for $D(\lambda)$ without significantly compromising the accuracy. First, the group index of the fiber core and cladding are assumed to have a similar variation with the wavelength making possible to estimate the composite material dispersion from (2). Second, the cladding refractive index variation with wavelength is ignored when evaluating $D_w(\lambda)$, as a result the waveguide dispersion can be approximated by (4).

$$D_w(\lambda) \approx -\frac{n_2 \Delta}{c\lambda}\left[V \frac{\partial^2(bV)}{\partial V^2}\right]. \tag{4}$$

In (4) n_2 is the refractive index of the fiber cladding and Δ is the normalized index difference, and V and b are, respectively, the normalized frequency parameter and the normalized propagation constant.

A simple approximation to the expression between square brackets in (4) was found by Jeunhomme [16]

$$V \frac{\partial^2(bV)}{\partial V^2} \approx 0.080 + 0.549\left(2.834 - 2.405\frac{\lambda_c}{\lambda}\right)^2. \tag{5}$$

In (5) λ_c stands for the cutoff wavelength of the LP_{11} mode. A typical value for λ_c in single-mode fibers is 1.2 nm and in this case the error associated with the approximation done in (5) is less than 5% over the range $1200 < \lambda < 2200$ nm [16].

Finally the profile dispersion, which appears in expression (3), can in principle be neglected due to its smaller value when compared with the composite material and waveguide dispersion.

2.2. A simplified model for the chromatic dispersion

For practical purposes a heuristic expression, (6), is frequently used to extrapolate the chromatic expression in optical fibers from the zero dispersion wavelength and the dispersion slope at the zero dispersion wavelength.

$$D(\lambda) = \frac{S_0}{4}\left(\lambda - \frac{\lambda_0^4}{\lambda^3}\right). \tag{6}$$

In (6) S_0 stands for the dispersion slope at the zero dispersion wavelength and λ_0 is the zero dispersion wavelength.

For a single-mode fiber with a cutoff wavelength of 1200 nm and a normalized index difference of 0.3% we obtained a maximum error of 6% for the dispersion value over the range $1200 < \lambda < 1700$ nm, when comparing the result obtained with the use of expressions (1) through

(5) with the result obtained with expression (6). The comparison of these values is plotted in Fig. 1.

The experimental validation of expression (6) was done in [13] for a wide range of single-mode optical fibers, commercially available and with practical interest for high speed optical communication systems. The results obtained with expression (6) matched the laboratory measurements considering the experimental uncertainty in the measurements, over a range of temperatures from −40 to 60 °C.

3. The temperature dependent dispersion and dispersion slope

In the previous section, we did not consider the effect of temperature. In this section, we are going to consider the temperature effect using two different approaches. The first approach will be based on the detailed model for the dispersion presented in Section 2.1 and the second on the simplified model for the dispersion presented in Section 2.2.

3.1. Based on the detailed model for the dispersion

It is known that the refractive index changes with temperature, which means that the A_k and

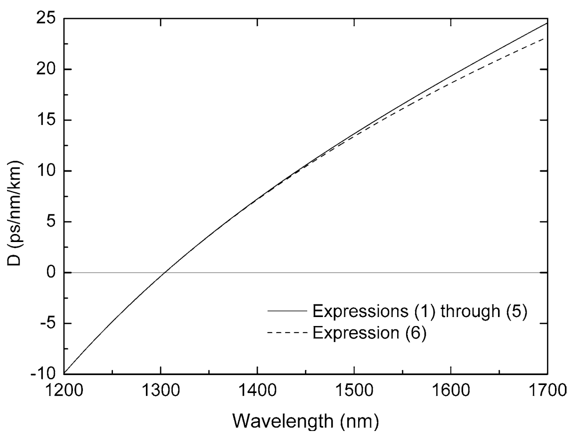

Fig. 1. Comparison between the dispersion values for a single-mode optical fiber obtained with expressions (1) through (5) and with expression (6). The S_0 and λ_0 parameters that appear in (6) where obtained considering the results of expressions (1) through (5).

λ_k coefficients, in expression (1), are temperature dependent. As the refractive index is temperature dependent, the dispersion and dispersion slope will also change with temperature. In order to model the dispersion and dispersion slope dependency of temperature we are going to analyze first the variation of the refractive index with temperature.

Expression (1) can be rewritten in terms of photon energies, doing this expression (7) is obtained.

$$n^2 = 1 + \sum_{k=1}^{m} \frac{a_k}{E_k^2 - E^2}. \tag{7}$$

In expression (7), E is the photon energy, E_k and a_k, are, respectively, the kth resonance energy and the oscillator strength multiplied by the number of oscillators per unit of volume correspondent to the kth resonance energy.

In [5], Matsuoka et al. presented the following values for the silica resonance energies: 0.14, 10.4 and 11.6 eV. The two resonance energies in the ultraviolet are related to electronic transitions and, since they are very close together can be lumped into one effective electronic resonance energy. In this way, the summation that appears in expression (7) is reduced to a two term summation, one to accounts for the lattice vibrations and another to describe the electronic transitions. Moreover, in [5] it was shown that the resonance energy around 0.14 eV, corresponds to a lattice vibration and is almost independent of the temperature.

Taking the derivative of (7) with respect to temperature and treating the term related to lattice vibrations as temperature independent, expression (8) is obtained

$$2 \cdot n \cdot \frac{\mathrm{d}n}{\mathrm{d}T} = \frac{1}{\left(E_\mathrm{e}^2 - E^2\right)} \frac{\mathrm{d}a_\mathrm{e}}{\mathrm{d}T} - \frac{2 a_\mathrm{e} E_\mathrm{e}}{\left(E_\mathrm{e}^2 - E^2\right)^2} \frac{\mathrm{d}E_\mathrm{e}}{\mathrm{d}T}. \tag{8}$$

In (8), the a_e coefficient is the product of the effective electronic oscillator strength by the number of oscillators per unit of volume and E_e is the effective resonance energy associated with the electronic transitions.

The oscillator strength can be assumed temperature independent, because the strength of an electrical oscillator is related with the mass and charge of the particles involved which are believed not to be significantly affected by temperature. In a different way the number of oscillators per unit of volume is temperature dependent because of the material thermal expansion. The material thermal expansion will decrease the number of oscillators per unit of volume by a factor that is approximately proportional to three times the linear thermal expansion coefficient.

Considering the linear thermal expansion coefficient, α, in (8) expression (9) is obtained.

$$2 \cdot n \cdot \frac{\mathrm{d}n}{\mathrm{d}T} = -\frac{3\alpha a_\mathrm{e}}{\left(E_\mathrm{e}^2 - E^2\right)} - \frac{2a_\mathrm{e}E_\mathrm{e}}{\left(E_\mathrm{e}^2 - E^2\right)^2}\frac{\mathrm{d}E_\mathrm{e}}{\mathrm{d}T}. \tag{9}$$

Expression (9) can be rewritten in order to introduce the n_1 parameter that appears in [7]. This n_1 parameter is the refractive index in a region of the spectrum between the two major resonance frequencies, the ionic and the electronic. In this region, the index of refraction already falls after the surge due to the ionic resonance and does not start to rise yet due to the electronic resonance, therefore is almost independent of the frequency. Introducing n_1 in expression (9) expression (10) is obtained.

$$\begin{aligned} 2 \cdot n \cdot \frac{\mathrm{d}n}{\mathrm{d}T} &= -3\alpha \frac{E_\mathrm{e}^2}{\left(E_\mathrm{e}^2 - E^2\right)}\left(n_1^2 - 1\right) \\ &\quad - \frac{E_\mathrm{e}^4}{\left(E_\mathrm{e}^2 - E^2\right)^2}\frac{2}{E_\mathrm{e}}\frac{\mathrm{d}E_\mathrm{e}}{\mathrm{d}T}\left(n_1^2 - 1\right). \end{aligned} \tag{10}$$

When expression (10) is rewritten in terms of the wavelength, expression (11) is obtained which corresponds precisely to expression (2) presented in [7].

$$\begin{aligned} 2n\left(\frac{\mathrm{d}n}{\mathrm{d}T}\right) &= \left(-3\alpha\left(n_1^2 - 1\right)\right)\left(\frac{\lambda^2}{\lambda^2 - \lambda_\mathrm{e}^2}\right) \\ &\quad + \left(-\frac{2}{E_\mathrm{e}}\frac{\mathrm{d}E_\mathrm{e}}{\mathrm{d}T}\left(n_1^2 - 1\right)\right)\left(\frac{\lambda^2}{\lambda^2 - \lambda_\mathrm{e}^2}\right)^2. \end{aligned} \tag{11}$$

One way to include the effect of temperature in the study of fiber optic communication systems is to use expression (11) in conjugation with expressions (1)–(5).

This approach requires the knowledge of the fiber profile and the core and cladding material, or some other values from which the input values for Eqs. (1)–(5) and (11) can be estimated.

3.2. Based on the simplified model for dispersion

Another approach to account for fluctuations in the dispersion due to temperature is to include this effect directly in expression (6). Assuming that both parameters of expression (6), λ_0 and S_0, are temperature dependents, the dispersion as function of the temperature is given by (12).

$$\frac{\mathrm{d}D}{\mathrm{d}T} = \frac{1}{4}\left(\lambda - \frac{\lambda_0^4}{\lambda^3}\right)\frac{\mathrm{d}S_0}{\mathrm{d}T} - \frac{S_0\lambda_0^3}{\lambda^3}\frac{\mathrm{d}\lambda_0}{\mathrm{d}T}. \tag{12}$$

From (12) is possible to obtain the dispersion variation with temperature around λ_0, by making λ equals λ_0. This was done in [9] and [13] and expression (13) was obtained

$$\left.\frac{\mathrm{d}D}{\mathrm{d}T}\right|_{\lambda=\lambda_0} = -S_0\frac{\mathrm{d}\lambda_0}{\mathrm{d}T}. \tag{13}$$

Expression (12) is critical to assess the importance of the temperature in optical systems. However, for high-speed systems as important as the chromatic dispersion is the chromatic dispersion slope around the central wavelength.

The chromatic dispersion slope can be obtained from (6), taking the derivative in order to the wavelength, by which expression (14) is obtained.

$$\frac{\mathrm{d}D}{\mathrm{d}\lambda} = \frac{S_0}{4}\left(1 + 3\frac{\lambda_0^4}{\lambda^4}\right). \tag{14}$$

From (14) and assuming again that λ_0 and S_0 are function of temperature is possible to derive an expression for the variation of the dispersion slope with the temperature, see expression (15).

$$\frac{\mathrm{d}}{\mathrm{d}T}\frac{\mathrm{d}D}{\mathrm{d}\lambda} = \frac{1}{4}\left(1 + 3\frac{\lambda_0^4}{\lambda^4}\right)\frac{\mathrm{d}S_0}{\mathrm{d}T} + 3S_0\frac{\lambda_0^3}{\lambda^4}\frac{\mathrm{d}\lambda_0}{\mathrm{d}T}. \tag{15}$$

The use of expressions (12) and (15) requires the knowledge of four values, the zero dispersion wavelength and the dispersion slope at the zero dispersion wavelength and their variations with temperature. Again, with the available published data for fused silica based optical fibers it is not difficult to find values for these parameters.

3.3. Expressions validation

In [13] the accuracy of expression (6) over a temperature range of 100 °C, from −40 to 60 °C, was evaluated by means of laboratory measurements of the chromatic dispersion in standard single-mode fibers and non zero-dispersion-shifted fibers subjected to a temperature controlled environment. From those measurements the values for λ_0 and S_0 for single-mode fibers where estimated for different temperatures and compared with the values predicted by a model based on expression (11). The theoretical values matched the experimental results within the uncertainty of the measurements, therefore validating expression (11).

Considering the values presented in [13] for S_0, $\mathrm{d}\lambda_0/\mathrm{d}T$, $\mathrm{d}S_0/\mathrm{d}T$ and their uncertainties, for a standard single mode fiber with the zero dispersion wavelength at 1319.30 ± 0.14 nm, at room temperature, and using expression (6) and (12) we estimated the fiber dispersion for different temperatures at 1550 nm. These values are plotted in Fig. 2, along with side error bars obtained by a standard-error propagation method. From this values a linear regression was obtained, dashed line. This result was compared with the one obtained using the detailed method presented in Section 3.1, solid line. As it is clear from Fig. 2, both methods led to similar results. A value of -1.4×10^{-3} ps/nm/km/°C was obtained for the chromatic dispersion thermal coefficient.

The dispersion slope for different temperatures was estimated using expression (14) and (15) and the values measured in [13], see the points in Fig. 3. Along side with these values an error bar is obtained using a standard error propagation method and the uncertainty in the measurements. After performing a linear regression a straight line with positive slope was obtained for the variation of the dispersion slope with temperature. The slope value obtained was 2.1×10^{-6} ps/nm^2/km/°C, see dashed line in Fig. 3. We also estimated the dispersion slope thermal coefficient using the detailed method presented in Section 3.1, with input parameters from [7], see full line in Fig. 3. As can be seen in Fig. 3, the obtained results are quite similar, confirming that both methods give results within the uncertainty of the experimental measurements.

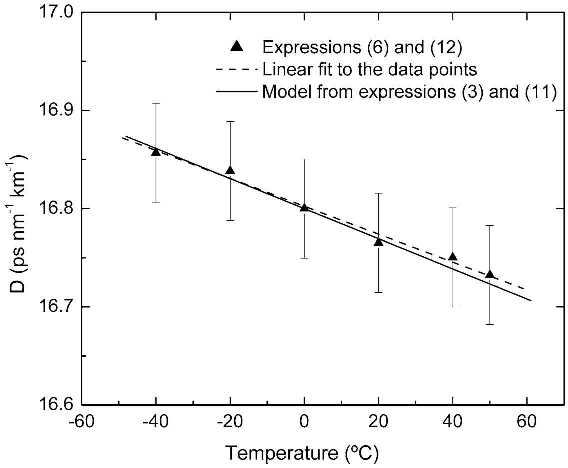

Fig. 2. Fiber chromatic dispersion as function of the temperature for 1550 nm. Points and error bars obtained using expression (6) and (12) with input parameters taken from [13] for a standard single-mode fiber with zero dispersion wavelength of 1319.30 ± 0.14 nm at room temperature. Dashed lines were obtained using a least-square error method applied to the plotted points. The solid line was obtained with expression (3) and (11), using input parameters obtained from [7].

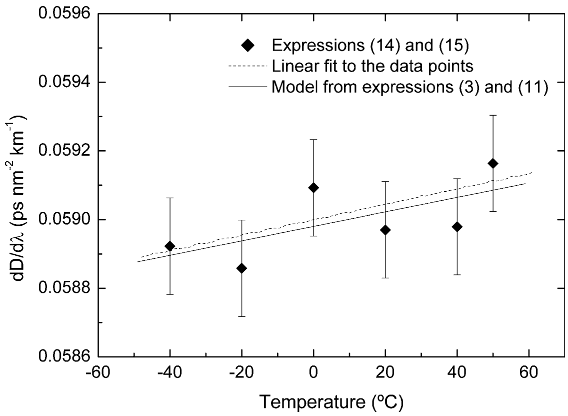

Fig. 3. Fiber chromatic dispersion slope as function of the temperature for 1550 nm. Points and error bars obtained using expression (14) and (15) with input parameters taken from [13] for a standard single-mode fiber with zero dispersion wavelength of 1319.30 ± 0.14 nm at room temperature. Dashed lines were obtained using a least-square error method applied to the plotted points. The solid line was obtained after calculating the numerical derivative in order to the wavelength of (3), using (11) with input parameters obtained from [7].

In this section, two different approaches were presented to include the temperature effect in the chromatic dispersion. Both methods give quite similar results and within the experimental uncertainty of the experimental values available. Therefore, the choice between one of them should be related with the kind and uncertainty of the available data for the optical link under analyze.

4. Implication in high speed systems

In order to evaluate the implications of the temperature effects in high speed systems, we analyzed several systems over the same optical link. The link that we considered was 500 km long, with five erbium doped fiber amplifiers (EDFA) spaced 100 km apart and being the first one placed just after the emitter to serve as a booster amplifier.

The emitter output pulses have a Gaussian shape with a FWHM width of 20% of the bit time slot, a 1550 nm central wavelength and the fiber is feed with an average power of +5 dBm. In the simulations, we solved numerically the generalized Schrodinger equation with the split step method [17], considering a pseudorandom bit sequence (PRBS) of $2^9 - 1$ word length.

Before the receiver the chromatic dispersion was optically compensated using DCFs in a scheme coined all-at-the-end [1]. The DCFs were assumed to fully compensate the optical link dispersion at the temperature of 20 °C for the employed wavelength, along with the DCFs links were intercalated ten optical amplifiers to compensate the losses. These amplifiers were used to compensated for losses in the DCFs and to keep the optical power in the DCFs at a reasonably level, 0 dBm at the DCFs input, in order to simultaneously prevent severe non-linear degradations and noise addition to the signal, as suggested in [1]. The DCFs and these ten amplifiers are assumed to be placed in a room along with the receiver in a controlled temperature environment. All the used EDFAs were ideal with a inversion population factor of $N_{sp} = 2$.

The optical receiver was modeled as an ideal PIN photodiode followed by a fourth-order Bessel–Thomson electrical filter. The electrical filter bandwidth at the receiver was adjusted for each system in order to remove part of the noise without producing a severe intersymbolic interference. This resulted in a value for the electrical filter bandwidth around 0.8 of the bitrate. Each system was optimized for 20 °C outside temperature in terms of eye open aperture. After the optimization the outside temperature was allowed to change and the eye open aperture was measured for different temperatures. The eye open penalty was defined as conventionally, see expression (16), where $\mathrm{EOA}_{20\,°\mathrm{C}}$ stands for eye open aperture at 20 °C and EOA_T for the eye open aperture at a temperature T.

$$P = -10 \cdot \log_{10}\left(\frac{\mathrm{EOA}_T}{\mathrm{EOA}_{20\,°\mathrm{C}}}\right). \tag{16}$$

The obtained results are presented in Fig. 4. As it is clear from these results, the 10 Gbit/s system is almost insensitive to temperature changes. However the 40 and 80 Gbit/s systems suffer a considerable penalty due to temperature change, analogous results for this two bit-rates were presented in [14] and [15], respectively. The 160 Gbit/s system suffer a severe penalty with the temperature change, a 3.8 °C drift in the temperature produces a 3 dB penalty.

The asymmetry of the penalty in relation to the optimized point, clearly visible in the 40 Gbit/s data, demonstrate that the all-at-the-end compensation scheme is more tolerant to positive overall

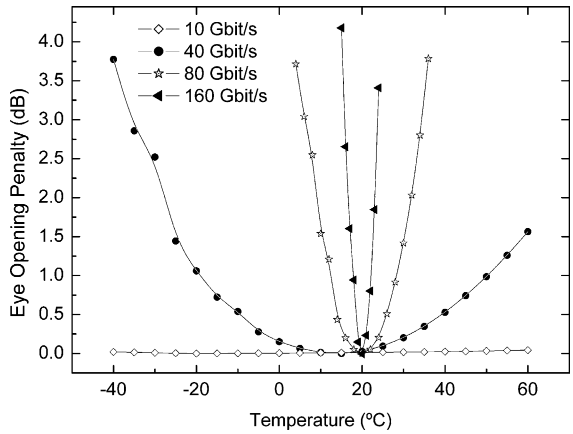

Fig. 4. Eye opening penalty versus temperature of the optical fiber link for several system bitrates. All systems were optimized for a 20 °C environment temperature. Lines are guides for the eyes. Results obtained for 500 km of fiber, ideally dispersion compensated at 20 °C, employing Gaussian optical pulses with a pulse width of 20% of the bit time slot.

dispersion than to negative overall dispersion. At 40 Gbit/s, according to several field trial results presented in the literature, it seems possible to compensate this penalty by means of forward error correction codes but at 160 Gbit/s the penalty is so high that it seems infeasible to compensate that by coding. In these high speed systems seems that some kind of dynamically adjustable receiver must be used in order to compensate the effect of temperature.

5. Conclusions

Two different methods to account for the thermal effect in optical fibers were presented. The methods were compared and assessed by means of comparison with measured values. Both methods produce results within the experimental uncertainty. Some high speed systems were analyzed for thermal sensitivity. Systems at 40 Gbit/s and above presented a severe degradation due to temperature changes. A sweep of temperature between −40 and 60 °C was considered. Aerial optical systems are expected to suffer changes of temperature of this magnitude in several areas of the planet, which enforce the need to consider the thermal effect in the design of high speed optical communication systems. In the case of underground systems, daily soil temperature changes are small, however seasonal variations could be considerable, as was shown by Walter et al. [18], making again critical to consider this effect in high speed systems design. In undersea systems, which operate in a more controlled environment, the fact that systems assembly and test usually take place at room temperature may indicate the need for use of an adjustable receiver to compensate the temperature difference between the laboratory and the deep ocean. In the analyzed systems the DCFs fibers were kept inside a room along with the optical amplifiers and receiver, this is a typical procedure; however with respect to temperature sensitivity same improvement could be achieved with positive dispersion thermal coefficient DCF fibers if there temperature is kept more correlated with the transmission fibers temperature.

Acknowledgements

The authors are grateful to Prof. Govind Agrawal and Prof. Ferreira da Rocha, for critical reading of the manuscript and suggestions. This work was supported in part by the Portuguese Scientific Foundation, FCT, through the DOPTNET project (POSI/CPS/42073/2001), FEDER and POSI programs.

References

[1] Anna Pizzinat, Alessandro Schiffini, Francesco Alberti, Francesco Matera, Armando N. Pinto, Paulo Almeida, IEEE/OSA J. Lightwave Technol. 20 (2002) 1673.
[2] William Hatton, Masayuki Nishimura, IEEE/OSA J. Lightwave Technol. 4 (1986) 1552.
[3] Kwang S. Kim, M.E. Lines, J. Appl. Phys. 73 (1993) 2069.
[4] M.E. Lines, J. Appl. Phys. 73 (1993) 2075.
[5] J. Matsuoka, N. Kitamura, S. Fujinaga, T. Kitaoka, H. Yamashita, J. Non-Crystalline Solids (1991) 86.
[6] Gorachand Ghosh, Michiyuki Endo, Takashi Iwasaki, IEEE/OSA J. Lightwave Technol. 12 (1994) 1338.
[7] Gorachand Ghosh, IEEE Photon. Technol. Lett. 6 (1994) 431.
[8] Gorachand Ghosh, Handbook of Thermo-Optic Coefficients of Optical Materials with Applications, Academic Press, New York, 1998.
[9] T. Kato, Y. Koyano, N. Nishimura, Opt. Lett. 25 (2000) 1156.
[10] V.M. Schneider, Electron. Lett. 37 (2001).
[11] J. Rathje, M. Andersen, Opt. Fiber Commun. Conf. 2 (2003) 712.
[12] P.S. André, B. Neto, R. Nogueira, J.L. Pinto, A.L.J. Teixeira, A.N. Pinto, M.J. Lima, F. Da Rocha, in: Conference on Lasers and Electro Optics/International Quantum Electronics Conference, CLEO/IQEC'2004, San Francisco, USA, 2004.
[13] Michael J. Hamp, John Wrigtht, Michael Hubbard, Bob Brimacombe, IEEE Photon. Technol. Lett. 14 (2002) 1524.
[14] P.S. André, A.N. Pinto, J.L. Pinto, in: SBMO/IEEE MTT-S International Microwave and Optoelectronics Conference, IMOC'03, Foz do Iguazu, Brazil, 2003.
[15] P.S. André, A.N. Pinto, in: The 16th Annual Meeting of the IEEE Lasers and Electro-Optics Society, LEOS'03, Tucson, USA, 2003.
[16] John A. Buck, Fundamentals of Optical Fibers, Wiley Series in Pure and Applied Optics, 1995.
[17] G.P. Agrawal, Nonlinear Fiber Optics, Academic Press, San Diego, CA, 1995.
[18] Alexander Walter, Garry Schaefer, Opt. Fiber Commun. Conf. (2002) 332.